ORIGINAL PAPER

Check for updates

Formation and decay of peat bogs in the vegetable belt of Switzerland

Markus Egli[1][*] , Guido Wiesenberg[1], Jens Leifeld[2], Holger Gärtner[3], Jan Seibert[1], Claudia Röösli[1], Vladimir Wingate[1], Wasja Dollenmeier[1], Pascal Griffel[1], Jeannine Suremann[1], Jan Weber[1], Mergime Zyberaj[1] and Alessandra Musso[1]

Abstract

The rapidly collapsing glacial systems of the Alps produced a large number of melt-water lakes and mires after the Last Glacial Maximum (LGM) in the Late Glacial period. The Rhone-Aare-glacier system gave rise to large moorlands and lakes in the region of the Three Lakes Region of Western Switzerland. When moorlands are formed, they are efficient sinks of atmospheric carbon, but when transformed to agricultural land they are significant C sources. In addition, mires can be used as archives for reconstructing landscape evolution. We explored in more detail the dynamics of the landscape of the Three Lakes Region with a particular focus on the formation and degradation of mires. The Bernese part of the Three Lakes Region developed to become—after the optimisation of the water-levels of the Swiss Jura—the vegetable belt of Switzerland. The situation for agriculture, however, has now become critical due to an overexploitation of the peatland. Until c. 13 ka BP the entire region was hydrologically connected. An additional lake existed at the western end of the plain receiving sediments from the Aare river. Around 13 ka BP, this lake was isolated from the Aare river and completely silted up until c. 10 ka BP when a mire started to form. In the valley floor ('Grosses Moos'), the meandering Aare and the varying level of the nearby lake of Neuchâtel caused a spatio-temporally patchy formation of mires (start of formation: 10–3 ka BP). Strong morphodynamics having high erosion and sedimentation rates and a high variability of the chemical composition of the deposited material prevailed during the early Holocene until c. 7.5 ka BP. The situation remained relatively quiet between 5 and 2 ka BP. However, during the last 2000 years the hydrodynamic and geomorphic activities have increased again. The optimisation of the Swiss Jura water-levels during the nineteenth and twentieth centuries enabled the transformation of moorland into arable land. As a consequence, the moorland strongly degraded. Mean annual C-losses in agricultural land are c. 4.9 t ha^{-1} and c. 2.4 t ha^{-1} in forests. Because forests limit, but not stop, the degradation of mires, agroforestry might be tested and propagated in future as alternative land-use systems for such sensitive areas.

Keywords: Landscape evolution, Mire degradation, C-losses, Holocene, Sedimentation, Land-use change

1 Introduction

It is commonly known that mires (having living peat-forming plants) and peatlands (terrain dominated by peat) that globally cover c. 3% of the land surface

*Correspondence: markus.egli@geo.uzh.ch
[1] Department of Geography, University of Zürich, 8057 Zurich, Switzerland
Full list of author information is available at the end of the article

(Limpens et al. [2008]) are efficient sinks of carbon as in these environments, under mostly anaerobic conditions, organic matter is accumulated (Leifeld et al. [2020]). Degradation of organic substances is very slow under these environmental conditions. In intact peat bogs, peat is transformed with age. This may be observed by the decreasing C/N ratios with depth (Malmer and Holm [1984]; Wang et al. [2015]; Leifeld et al. [2020]), but changing vegetation with time and developing environmental settings may overshadow this trend. This situation is

fundamentally disturbed when the mires are drained and used for agricultural purposes that ultimately lead to an increased peat decomposition. Therefore, when mires are drained and, thereafter, converted into agricultural land, the former C-sink transforms into a strong C-source. Over the last century, more than 50% of the peatland area in Europe has been converted mainly into land used for agriculture or forestry (Byrne et al. 2004). Particularly in northern countries, former peatland was drained and converted for sylviculture purposes (Hargreaves et al. 2003; Pitkänen et al. 2012). For example, in Switzerland, a large proportion of mires and peatland were transformed for sylvicultural purposes, although the total area is small compared to the land transformed for agricultural purposes (Grünig 2007; Wüst-Galley et al. 2020).

Mires and peatland register environmental history and changing ecological and climatic conditions. In effect, the age of organic matter, pollen and macrofossils are often-used parameters for palaeoenvironmental reconstructions of the Late Pleistocene and Holocene (e.g., Burga and Perret 1998; Birks and Birks 2001; Tinner and Theurillat 2003; Zanon et al. 2018), however, less attention has been given to the chemical signature of mires to trace environmental changes (e.g., Mourier et al. 2010; Bajard et al. 2017). As such, recent approaches have examined the links between the chemical composition of mires and surrounding soils or sediments to trace the origin of lateral input (e.g., Brisset et al. 2013; Bajard et al. 2017).

In the late Pleistocene, deglaciation of the Alps began by 21 ka BP (Ivy-Ochs et al. 2006). The rapidly collapsing glaciers at the end of the Last Glacial Maximum (Preusser 2004; Schlüchter 2004; Ivy-Ochs et al. 2006) produced a vast number of small melt-water lakes, kettles and mires in the Swiss Alpine foreland. The accumulating lacustrine clays, muds and peat layers trapped signals of the on-going landscape development and preserved them as environmental archives across peatlands and mires (Jäger et al. 2015).

The recent degradation of peatlands and mires is caused by several factors; among them are (i) the draining of the area and the resulting desiccation of the peat, (ii) the use of fertilisers accelerating decomposition, (iii) agriculture (e.g. ploughing) and silvicultural use, and (iv) atmospheric nitrogen deposition (Klaus 2007).

In Switzerland, the remaining intact or semi-intact moorlands in general have been protected since 1987 whereas this is not the case for the managed peat soils. As the Rhone-Aare-glacier retreated at the end of the last glaciation, vast moorlands started to develop in the Bernese Swiss Plateau (Three Lakes Region). During the nineteenth and twentieth centuries, the optimisation of the water-levels of the Swiss Jura allowed to transform the peatlands and mires of this area into arable land. These measures enabled a productive agriculture and the Three Lakes Region became the main vegetable producer in Switzerland (Nast 2006). Due to the intensive land use of mires, the peat soils have shrunk drastically over the last 100 to 150 years, with the effect that in several parts of the area only a thin 'soil' layer (10–20 cm), mainly consisting of degraded organic material, exists on top of lake marls or clays (Zihlmann et al. 2019). In order to establish a more sustainable use of this area while maintaining its productivity, basic data about the formation of these mires and their degradation are needed. As a consequence, this study proposed the following research questions: (i) when and how did the mires start to form?, (ii) which climatic-environmental signals can be deciphered since then and (iii) at which rate did and do the mires degrade?

2 Study area

The Three Lakes Region in Western Switzerland includes the area having the lakes of Murten, Biel and Neuchâtel in the lowlands in front of the Jura mountains (Fig. 1). The main plain between the lake of Neuchâtel, lake of Biel and Aarberg is the 'Grosses Moos' (the great marsh). The Tree Lakes Region is part of the Swiss plateau that is one of the major landscapes of Switzerland situated between the Jura mountains to the West and the Swiss Alps to the East. The climate today is temperate (having a mean annual temperature of 8.5–10 °C and mean annual precipitation of c. 1000–1200 mm; https://www.meteoschweiz.admin.ch/home/klima/klima-der-schweiz/jahresverlauf-temperatur-sonne-niederschlag.html). In its basal part, the Swiss Plateau is built up of sand- and siltstones, marls and conglomerates (Nagelfluh) of the Molasse. These geological units are widely covered by Pleistocene sediments of different origin, mainly till and glaciofluvial outwash deposits (gravel and sand), reworked with loess (Veit et al. 2017). The topography of this area has been repeatedly modified by glacier advances during the Pleistocene. The Rhone-Aare glacier system (coming from the Alps) reached its maximum during early Marine Isotope Stage (MIS) 2, probably at c. 24–27 ka (Preusser et al. 2007; Ivy-Ochs et al. 2008) near Aarwangen (to the north-east of Wangen a. A., Fig. 2). Readvances of this glacial system occurred at c. 20.7 and 19 ka (Wüthrich et al. 2018). During these readvances, the Aare glacier reached the position of Bern and the Rhone-glacier of Solothurn (Veit et al. 2017). Due to the repeated glacier advances, the bedrock was eroded to great depths and later refilled with sediments (Fig. 2). These quaternary sediment deposits down to the polished bedrock have a thickness of up to 300 m. At the top, mires have been
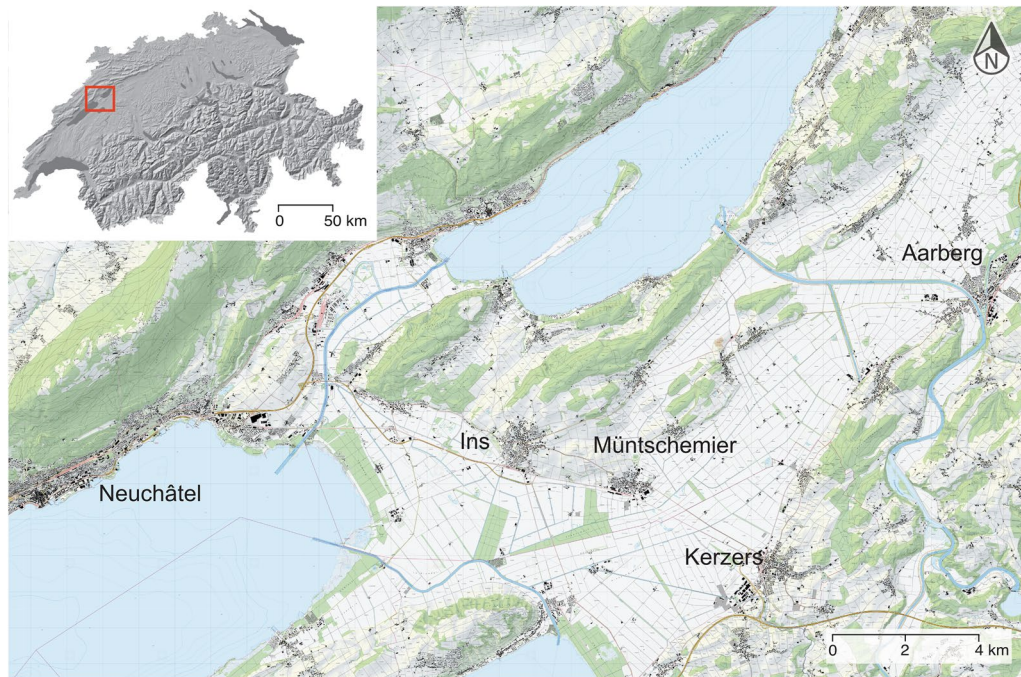
Fig. 1 Part of the Three Lakes Region of Western Switzerland. The area of interest lies between the Lake of Neuchâtel and Aarberg (Source: LK 25 swisstopo). The main plain between Ins, Kerzers and Aarberg is the 'Grosses Moos'
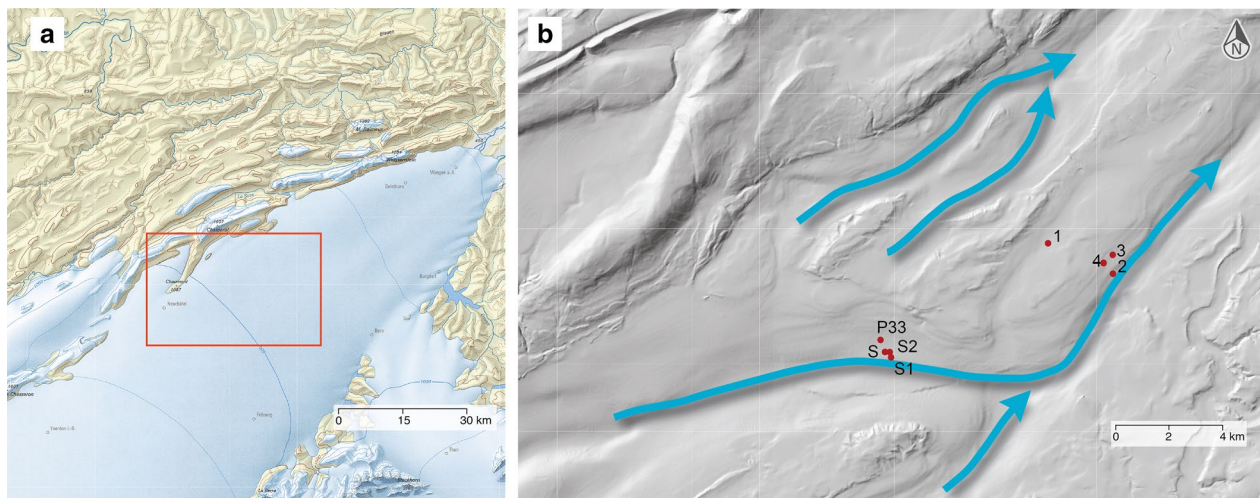

Fig. 2 **a** Extension of the Rhone-Aare-glacier system during the Last Glacial Maximum (LGM) in the study area. **b** Detail of the map (**a**) with topographic hillshade of the bedrock (bedrock elevation model) showing the former melt-water channels (blue arrows; Source: swisstopo) together with investigated profiles (for details, see Fig. 4)

covering a large part of the Three Lakes Region and usually reached a thickness of a few metres.

The Aare river influenced the hydrology and morphology of the landscape distinctly. It drained oftentimes in direction to the Lake of Neuchâtel fr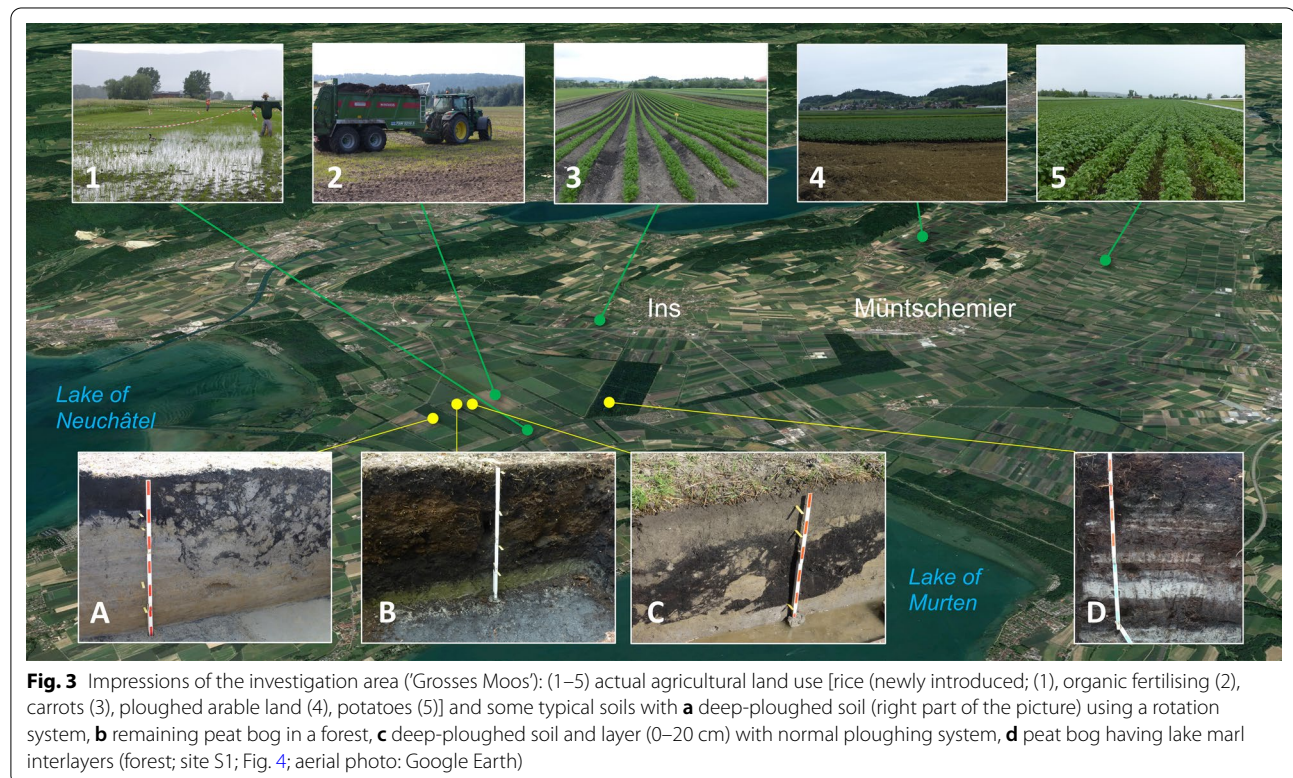om 11 to 5 kyr BP and since then mostly to the north (Wohlfarth-Meyer 1987). Until c. 160 years ago, floods, diseases (malaria) and poverty determined the life of the local population. The first intervention to regulate the water-levels of the Swiss Jura (1868–1897) included a number of technical hydrological measures to control the river Aare, the water table of the lakes and in

general to regulate the hydrological conditions of the region (Vischer and Feldmann 2005). These measures markedly improved the situation for the local population and as a result a productive agriculture could be established. In the twentieth century, however, various problems and new floods occurred again due to surface subsidence across large areas caused by mineralisation of organic matter in soils. As a consequence, a second optimisation of the water-levels of the Swiss Jura (1962–1973) was necessary (Moser 1991), which improved the general situation. However, the degradation of the mires proceeded. Today, different types of Histosols and Fluvisols are found in the investigation area (Table 1). Generally, these peat dominated soils are degraded, but under forest vegetation, the former peat bogs are partially still recognisable (Fig. 3). On agricultural land, ploughing and in part deep ploughing is practiced to improve soil quality (e.g., mixing of organic with inorganic layers; Fig. 3) and thus prepare the fields for vegetable cultivation or for improving soil quality (e.g. mixing of organic with inorganic layers; Fig. 3). Due to the degradation via mineralisation of organic matter of the soils, alternative types of agriculture are now being explored (e.g. rice cultivation).

Table 1 Characteristics of the sampling sites

Site	Coordinates		Altitude	Land use	Soil type (IUSS Working Group WRB 2014)
	°N	°E	m a.s.l		
1	47° 02′ 06″	7° 10′ 22″	438	Agriculture land (vegetables)	Folic Histosol
2	47° 01′ 32″	7° 12′ 19″	439	Agriculture land (vegetables)	Histic Fluvisol
3	47° 01′ 49″	7° 12′ 09″	439	Agriculture land (vegetables)	Skeletic Fluvisol Humic
4	47° 01′ 45″	7° 12′ 03″	439	Agriculture land (vegetables)	Folic Fluvisol
S1	46° 58′ 57″	7° 05′ 33″	432	Forest (pine, spruce)	Fibric Histosol
S2	46° 59′ 06″	7° 05′ 34″	432	Forest (beech, larch)	Fibric Histosol
S	46° 59′ 06″	7° 05′ 23″	431	Agriculture land (vegetables)	Folic Histosol
P33	46° 59′ 13″	7° 05′ 05″	431	Agriculture land (vegetables)	Folic Histosol

Fig. 3 Impressions of the investigation area ('Grosses Moos'): (1–5) actual agricultural land use [rice (newly introduced; (1), organic fertilising (2), carrots (3), ploughed arable land (4), potatoes (5)] and some typical soils with **a** deep-ploughed soil (right part of the picture) using a rotation system, **b** remaining peat bog in a forest, **c** deep-ploughed soil and layer (0–20 cm) with normal ploughing system, **d** peat bog having lake marl interlayers (forest; site S1; Fig. 4; aerial photo: Google Earth)

3 Material and methods

3.1 Sampling strategy

Attempting to cover the variability of bogs in the study area, a total of 8 mire profiles were investigated; four of them were located close to the lake of Neuchâtel and the other 4 were located in the northern part of the former moorlands (Fig. 4). To better understand the processes and rates of surface subsidence, profiles in agricultural land and forests were chosen. Some areas were reforested towards the end of the nineteenth century (1876; "Staatswald" to the south of Ins, Fig. 4; Lienert 2013). Large pits having a depth of c. 2 m were dug using an excavator at the sites close to the Lake of Neuchâtel (Lienert 2013). Here the possibility was given to directly compare mires under agricultural and silvicultural use (Table 1). Sampling was done in 5 to 20 cm intervals with four replicates in each pit. Undisturbed samples were taken from the profile faces to determine bulk density. In addition, disturbed samples for physical and chemical analyses were taken.

At the other four sites, mires in agricultural land were sampled. In addition, these sites were in an ancient meandering area (2, 3, 4) of the Aare river, where the formation of the mires probably started at different times and was sporadically interrupted. One profile was sampled outside of this zone (profile 1) in an area where a former lake was assumed. We expected to find here a long and continuing chronology. The cores were sampled using a Humax rotating drill and a Russian side-opening sampler (Macaulay). The cores reached a depth of up to 5 m. These samples were taken in 10 cm intervals and used to determine bulk density and chemical properties. Profile 3 was previously classified as a 'stony' bog.

3.2 Chemical and physical analyses

Oven-dried samples (70 °C) were sieved to < 2 mm (fine earth) and homogenised. The bulk density (fine earth and soil skeleton) was measured on undisturbed samples (volumetric sampling using the corers and cylinders). Soil, sediment and peat pH (0.01 M CaCl$_2$) was determined using a soil:solution ratio of 1:2.5. Loss on ignition (LOI) was measured on 2.0 g oven-dried fine earth samples and combusted at 550 °C for 7 h.

The total elemental content (only for the profiles 1, 2 and 4) was determined by using energy dispersive X-ray fluorescence (ED-XRF). Approximately 5 g of material was milled to < 63 µm in a Tungsten carbide mill (Retsch® MM400, Germany) and analysed using an energy dispersive He-flushed X-ray fluorescence spectrometer (SPECTRO X-LAB 2000, SPECTRO Analytical Instruments, Germany). The total carbon (C) and nitrogen (N) contents were determined using elemental analysis isotope ratio mass spectrometry (EA-IRMS). The measurements were performed using a Thermo Fisher Scientific Flash HT Plus elemental analyser with SmartEA option equipped with a thermal conductivity detector
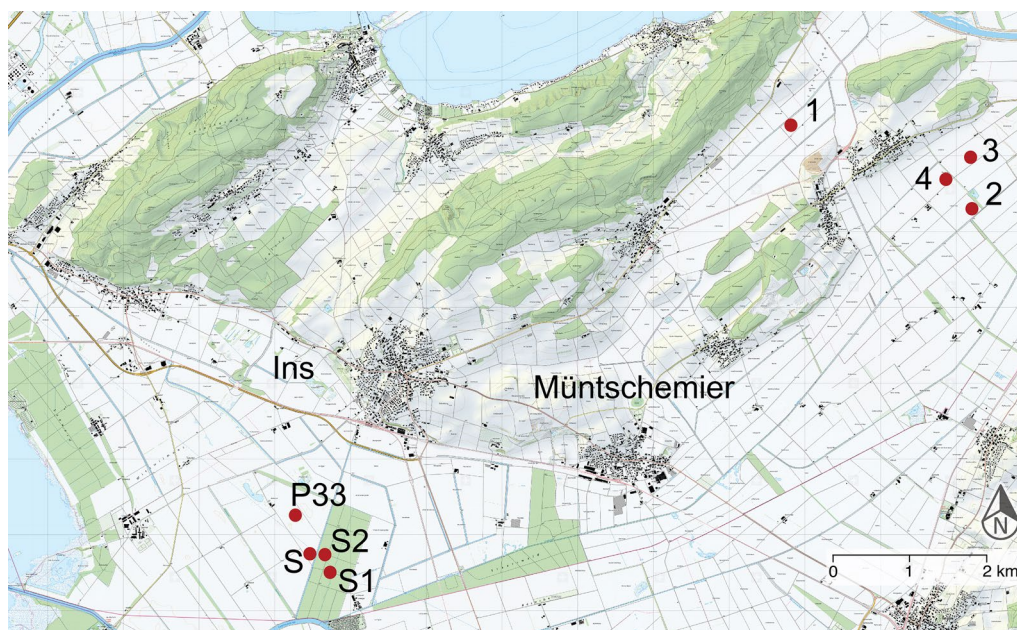

Fig. 4 Location of the investigated profiles. S1 and S2 are in a forest (Staatswald), P33 and S are in the adjacent agricultural land (Lienert 2013). These sites lie within the former extension of Lake Neuchâtel. Site 1 is western of the main plain (Grosses Moos) in the area of a former lake. Sites 2–4 are in the main plain (Grosses Moos) that has been affected by the Aare river (Source: LK 25 swisstopo)

and coupled to a ConFlo lV to Delta V Plus isotope ratio mass spectrometer. In order to distinguish between inorganic and organic C, the samples were measured before and after addition of HCl (to remove the carbonates). The measurements were carried out in duplicates.

3.3 Weathering and geoforensics

To characterise mineral alteration and chemical weathering in soils and sediments, several indices were used. These indices should also help in tracing the origin of the deposited material. Among them were the weathering index CIA (Chemical Index of Alteration), given as the molar ratio of $[Al_2O_3/(Al_2O_3 + CaO + Na_2O + K_2O)] \times 100$ (Nesbitt and Young 1982), the molar ratio of $(K + Ca)/Ti$ with Ti being the immobile element (Stiles et al. 2003), K and Ca the weatherable elements and $(K + Na)/Ti$ in order to overcome potential difficulties when using Ca and attributing it to carbonates or silicates.

In addition, the trace compound composition of the samples was compared to the primitive mantle (Sun and McDonough 1989). As demonstrated by Raab et al. (2017) or Derakhshan-Babaei et al. (2020), this procedure helps to identify the source of the deposited material or the connection between different sites.

3.4 Radiocarbon dating

By hand-picking, organic remains were depicted from the samples. The samples were then cleaned by an acid–alkali-acid (AAA) treatment. The treated material was combusted at 900 °C to produce CO_2 which was then reduced to graphite. The ratios of the carbon isotopes were measured by Accelerator Mass Spectrometry (AMS) using the 0.2 MV MICADAS facility at the Institute of Ion Beam Physics at the Swiss Federal Institute of Technology, Switzerland. The radiocarbon age calibration was done online using the OxCal4.3 tool using IntCal13 for calibration (Reimer et al. 2013). The calibrated ages are reported as calBP within the 2σ range (minimum and maximum value for each, Table 2).

3.5 Calculation of organic C losses

The degradation of peat and lowering of the surface is a twofold process. A first shrinking phase of the peat layer primarily includes only a compaction and no C loss. This shrinking is due to a lowering of the groundwater table and thus a water loss in the upper parts of the peat body. In a second step, peat or accumulated organic matter starts to decay. The whole process can be modelled using the approach presented by Leifeld et al. (2011). The method uses the ash, organic carbon content and bulk

Table 2 Characteristics and radiocarbon data of the investigated samples

ETH nr	UZ nr	Site	Depth (cm)	Material	^{14}C-age a BP	±1σ	F^{14}C[a]	±1σ	δ^{13}C (‰)	±1σ	Calibrated age cal BP (2σ)[b]
103108	6821	1	60–70	Peat	5765	25	0.488	0.00151	− 27.6	1.0	6493–6639
103109	6822	1	130–135	Peat	6665	26	0.436	0.00139	− 29.1	1.0	7491–7584
103110	6823	1	300–310	Shell	9759	28	0.297	0.00102	3.1	1.0	11,170–11,235
103111	6824	1	430–440	Organic residues	11,624	31	0.235	0.00090	− 30.4	1.0	13,393–13,561
103112	6825	2	60–70	Organic residues	4405	24	0.578	0.00171	− 30.0	1.0	4873–5044
103113	6826	2	170–180	Wood	5692	25	0.492	0.00152	− 28.1	1.0	6408–6536
103114	6827	3	30–40	Organic residues	3008	23	0.688	0.00196	− 25.9	1.0	3298–3093
103115	6828	3	60–65	Organic residues	− 91	21	1.011	0.00270	− 31.5	1.0	Modern
103116	6829	4	40–50	Organic residues	1836	22	0.796	0.00221	− 29.7	1.0	1710–1825
103117	6830	4	120–130	Snail shell	8504	27	0.347	0.00116	− 9.1	1.0	9479–9535
103118	6831	4	350–360	Organic residues	8707	27	0.338	0.00113	− 8.6	1.0	9553–9736
103119	6832	4	440–450	Organic residues	9073	28	0.323	0.00111	− 27.1	1.0	10,198–10,251
49291	6129	S1	80–95	Peat	6716	78	0.433	0.00419	− 23.5	1.1	7686–7440
49292	6130	S1	130–150	Peat	8958	101	0.328	0.00410	− 24.8	1.1	10,277–9697
49293	6131	S2	70–87	Peat	6555	78	0.442	0.00427	− 28.1	1.1	7580–7317
49294	6132	S2	120–145	Peat	9143	103	0.320	0.00408	− 24.9	1.1	10,647–9959
49295	6133	P33	75–85	Peat	8453	95	0.349	0.00410	− 24.2	1.1	9603–9141
49296	6134	P33	130–140	Peat	9479	108	0.307	0.00410	− 25.2	1.1	11,167–10,498
49289	6127	S	35–45	Peat	7168	83	0.410	0.00421	− 24.1	1.1	8173–7841
49290	6128	S	55–60	Peat	8464	96	0.349	0.00414	− 25.9	1.1	9659–9145

[a] Fraction modern carbon

[b] OxCal4.3, IntCal13 (Reimer et al. 2013)

density of the individual depth increments. The mass loss calculations are based on the simplified assumption of a constant ratio between organic matter and carbon to ash over the course of peat accumulation. A change in that ratio indicates respiratory losses of carbon as CO_2 induced by drainage and agricultural use (Leifeld et al. 2011). The first shrinking step can be calculated from:

$$\rho_{i,OS} = \rho_i F(1 - AS_i) \tag{1}$$

where AS_i = proportion of the ash content of layer i, ρ_i = bulk density (g cm^{-3}), $\rho_{i,OS}$ = density of organic matter (g cm^{-3}) and F = fine earth fraction. The former layer thickness $d_{i,f1}$ is given by:

$$d_{i,f1} = \left(\frac{\rho_{i,OS}}{\rho_{0,OS}} \right) \cdot d_i \tag{2}$$

where $\rho_{i,OS}$ = density of organic matter (g cm^{-3}), $\rho_{0,OS}$ = density of organic matter in the reference depth where no decay has occurred (g cm^{-3})—usually the lowermost peat layer. The sum of the first and second shrinking and sagging steps $d_{i,f2}$ (due to the degradation of organic matter) is calculated by using the ash content of the layer of interest (AS_i) and the reference layer (undisturbed situation; AS_0):

$$d_{i,f2} = \left(\frac{AS_i}{AS_0} \right) \cdot d_i \tag{3}$$

The loss of organic carbon can be estimated for each layer by using:

$$\Delta C(org)_i = \frac{C(org)_0}{d_0} \cdot \Delta d_i \tag{4}$$

where $\Delta C(org)_i$ = C-loss in the layer i (t ha^{-1}), d_o = thickness of the reference layer and Δd_i = volume loss of layer i.

4 Results

4.1 Stratigraphy, organic carbon content and physical parameters of the mires

The 8 mires have considerably different thicknesses (Fig. 5) with a maximum depth of up to 2.5 m and sometimes inorganic sediments are intercalated. The profiles S1, S2, P33 and S have peat and some lake marl interlayers. In profile 1, when listing the layers starting at the bottom, lacustrine clays were observed at a depth of 4.5 m and deeper. A layer of lake marls follows from 4.5 to 2 m depth. Between 2.5 and 2 m depth this layer becomes more organic giving rise to the formation of gyttja. The uppermost layer (2 m depth to the surface) consists of peat. The topmost 50 cm exhibit a slightly higher bulk density and are characterised by strongly

degraded organic material due to agricultural activities. Bulk density generally increases with depth at profile 2. Several layers can be discerned here as well. The lowermost layers consist of lacustrine clays that are intercalated by coarser material at a depth of 185 and 235 cm. An organic-rich layer is found from 75 cm depth to the surface. The upper 50 cm are strongly influenced by agriculture (higher density). At the site of profile 3 a 'stone-rich bog' (now a Skeletic Fluvisol) was found. This is the only site where a considerable amount of rock fragments (up to 87 weight-%) was captured. Although the soil material has a dark colour, the amount of c. 5% organic carbon was considerably low for a bog (Fig. 5). Due to its stoniness, it was not possible to drill deeper than 70 cm. Profile 4 has a relatively high amount of organic matter down to a depth of 65 cm. Between 65 and 335 cm follows a clay-rich layer and again a more organic rich layer below that is intercalated with coarser inorganic material.

4.2 Age—depth trends

A total of 20 samples from the eight mire cores were dated (Table 2). The age-depth trend for the uppermost 50 cm is quite similar at the sites 1–3 and S1 and S2. At a depth of c. 1.5 m, the profiles S, P33, S1, S2 and profile 4 reach an age of 9.5–11 ka cal BP (Fig. 6). These profiles show the strongest age-depth trend in the top 150 cm. After 150 cm, the ages increase only slightly with depth at profile 4. A maximum age of 13.5 ka cal BP was measured in the lake marl at profile 1 at a depth of c. 4.5 m. The shape of the age-depth trend however varies considerably showing that the mires developed differently (Fig. 6). This is due to the varying environmental settings at the different sites and also due to human impact.

4.3 Carbon losses and sedimentation/accretion rates

Due to the inhomogeneity of some profiles or the fact that they do not really represent a bog (e.g. profile 3), C-losses could only be determined for S, P33, S1, S2 and profile 1 (Fig. 7). The C-losses at the sites 1, S and P33 are quite similar, having average values of 4.58–5.04 t ha^{-1} year^{-1} (Fig. 8). The C-losses in the managed forest—having 2.36 t ha^{-1} year^{-1}—are distinctly lower (about half of those of the agricultural land). Consequently, forests do not fully maintain mires, but they reduce their degradation substantially. How the carbon losses distribute over a whole profile is given in Fig. 7 (for profile 1) where the carbon stocks prior to the optimisation of the water-levels of the Swiss Jura are plotted and compared to the present-day situation. The relating calculation procedure and results are given in Table 3. As shown in Fig. 7, the relation between subsidence and carbon loss is highly significant but not linear. Surface lowering of all investigated peat bogs ranged between 76 and 249 cm.
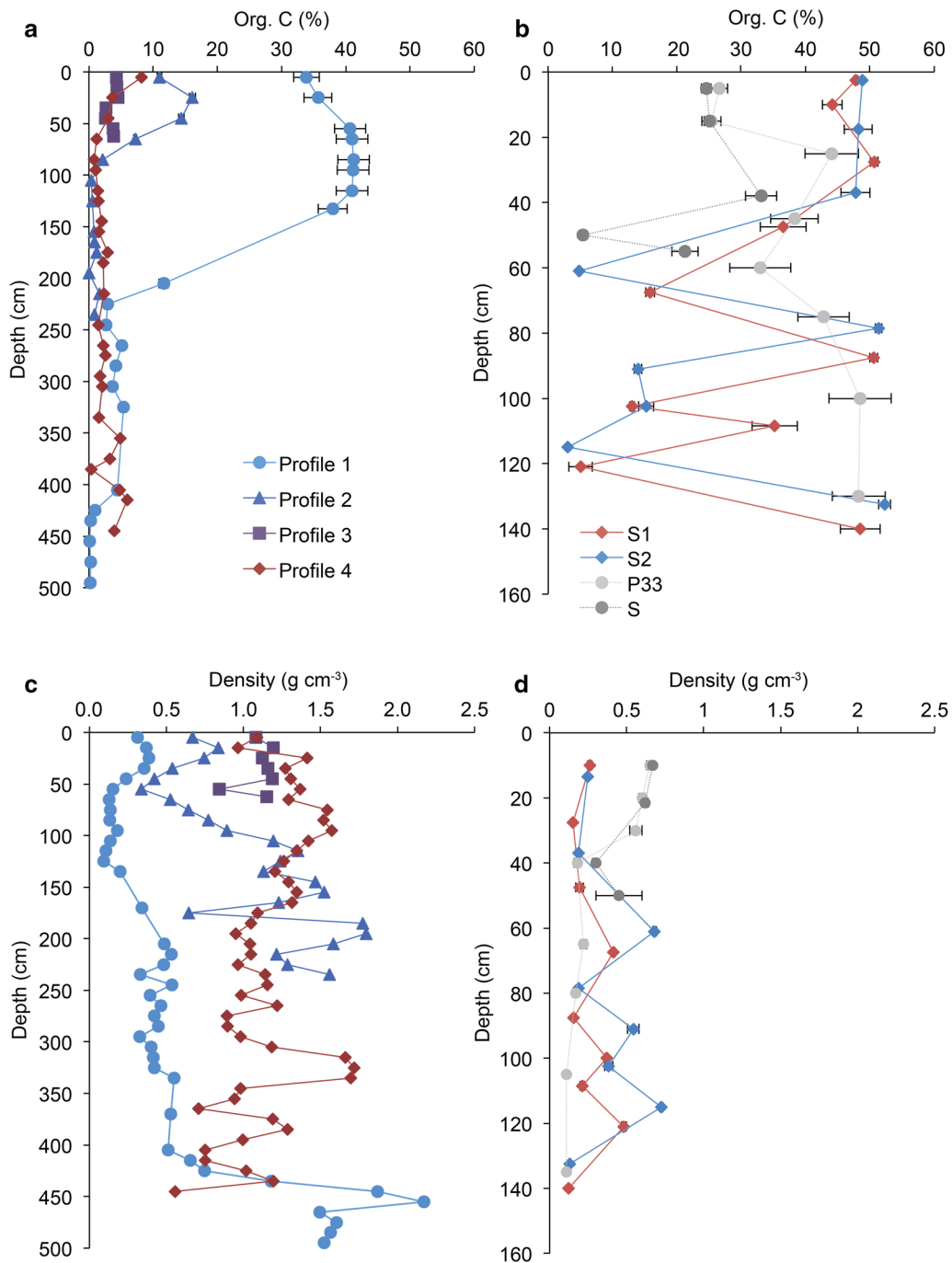
Fig. 5 Organic carbon content as a function of depth for **a** profiles 1–4, **b** S1, S2, P33, S and bulk density distribution at **c** profiles 1–4, **d** S1, S2, P33, S

Based on the depth-age trends, sedimentation or accretion rates at the investigated sites over time could be calculated. These rates are given in cm year^{-1} or, when considering the bulk density of the sedimented material, in t ha^{-1} year^{-1}. Profile 4 clearly indicates high deposition

rates at the transition from the Pleistocene to the Holocene. Furthermore, higher rates are recorded for the last c. 2 kyr. When considering Fig. 9, it can be recognised that this site was dominated by sediment inputs from the meandering Aare in the river plain (cf. Wohlfarth-Meyer

Fig. 6 Age-depth profiles (plotted using Clam; Blaauw 2010) of the investigated profiles with **a** profiles 1–4 (cf. Fig. 4) and **b** S1, S2, P33, S
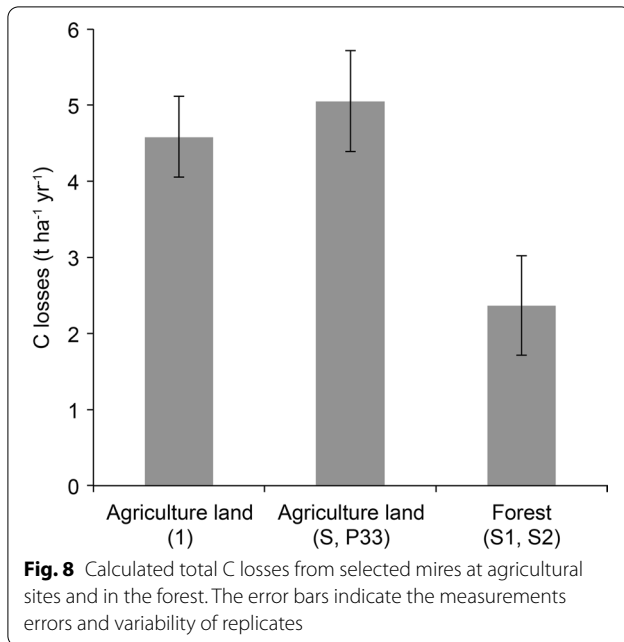

Fig. 7 a Present-day carbon stocks at profile 1 compared with the former stocks (prior to the Swiss Jura Water corrections), **b** calculated C-losses as a function of profile depth, **c** correlation between surface lowering and C-losses (all investigated sites)

1987) and only the top 30 cm and some interlayers have a slightly higher organic matter content. Profile 2 records approximately the 8 ka. Also, this profile is predominantly influenced by the former meandering Aare river. Higher sedimentation rates are recognised from c. 8–5 ka BP and then again for approximately last 2 ka. The entire profile 1 represents the sedimentation in a former lake. Again, highest sedimentation rates were measured at the

Pleistocene/Holocene transition. Then, from c. 10 ka BP a mire started to form.

4.4 Weathering and geoforensics

The chemical weathering and spidergrams reveal some interesting aspects (Fig. 10c, d). Profile 1 represents the geochemical situation of a lake and its close surroundings. The CIA and $(Ca + K)/Ti$ or $(Na + K)/Ti$ ratios show

Fig. 8 Calculated total C losses from selected mires at agricultural sites and in the forest. The error bars indicate the measurements errors and variability of replicates

deposition of more strongly weathered material. Since then, the $(Ca+K)/Ti$ or $(Na+K)/Ti$ values are higher and the CIA is lower, respectively. Fluctuations of the weathering indices are particularly discernible between 10 and 12 ka BP and later c. 8 ka BP. For approximately the last 6 ka, the indices remain in a similar range. Profile 4 represents more the situation of the valley floor having the former meandering Aare river. Similar to the sedimentation rates, a major disturbance is noted around 10 ka BP (Fig. 10). Additional minor changes seem to have occurred around 8 ka BP and c. 3.5 ka BP. It is interesting to note that the CIA and $(Ca+K)/Ti$ or $(Na+K)/Ti$ values are identical to those at profile 1 prior to 13 ka BP. Profile 1 showed strongly varying levels of incompatible trace element enrichment or depletion compared to the primitive mantle material. These values vary between 0.009 (lowest value of Zr) to 410 (highest value of U). This variability is much less pronounced at profile 4 where all samples exhibited a more or less similar trend over time. Until c. 13 ka BP, profile 1 exhibits exactly the same spidergram pattern as profile 4 (although a pattern could be calculated for this site only since 10 ka BP). This indicates that the origin of the deposited material is the same. Thus, the incompatible elements and weathering indices indicate a common source. This means that the

almost identical trends. A high CIA and low $(Ca+K)/Ti$ or $(Na+K)/Ti$ values indicate stronger weathering conditions. From 15 to c. 13–12 ka BP, the indices indicate the

Table 3 Calculation of organic matter (LOI) and C-losses of profile 1

Depth (cm)	LOI (%)	Bulk density (g cm^{-3})	Thickness (cm) (1)	Skeleton proportion (weight-%)	Density of organic matter (g cm^{-3})	Former thickness, primary subsidence (cm) (2)	Former thickness, primary and secondary subsidence (cm) (3)	LOI loss (kg m^{-2})	C-loss (kg m^{-2})
0–10	72.6	0.31	10	13	0.20	22.8	30.2	17.49	9.13
10–20	72.3	0.37	10	13	0.23	26.8	30.8	17.99	9.39
20–30	72.1	0.39	10	1	0.28	32.0	35.4	21.93	11.45
30–40	68.6	0.35	10	27	0.18	20.6	29.2	16.56	8.64
40–50	76.6	0.24	10	32	0.12	14.5	20.4	8.95	4.67
50–60	83.0	0.15	10	0	0.13	14.6	21.6	10.02	5.23
60–70	88.4	0.13	10	0	0.11	13.1	14.7	4.09	2.14
70–80	90.0	0.13	10	5	0.11	13.3	12.1	1.78	0.93
80–90	82.6	0.13	10	21	0.08	9.8	17.5	6.50	3.39
90–100	83.3	0.18	10	0	0.15	17.5	21.3	9.78	5.10
100–110	84.0	0.13	10	5	0.11	12.4	19.5	8.20	4.28
110–120	88.1	0.11	10	3	0.09	10.7	14.8	4.13	2.16
120–130	92.1	0.09	10	0	0.09	10.0	10.0	0	0
130–135	76.6	0.20	5	0	0.15	8.8	14.9	4.22	2.20
						Sum of difference (cm) = (2)—(1)	Sum of difference (cm) = (3)—(1)	Sum (kg m^{-2})	Sum (kg m^{-2})
						91.8	157.4	131.6	68.7

The average, annual C loss is calculated form the sum of C losses divided by 150 years (result = 0.458 kg m^{-2} year^{-1} = 4.58 t ha^{-1} year^{-1})
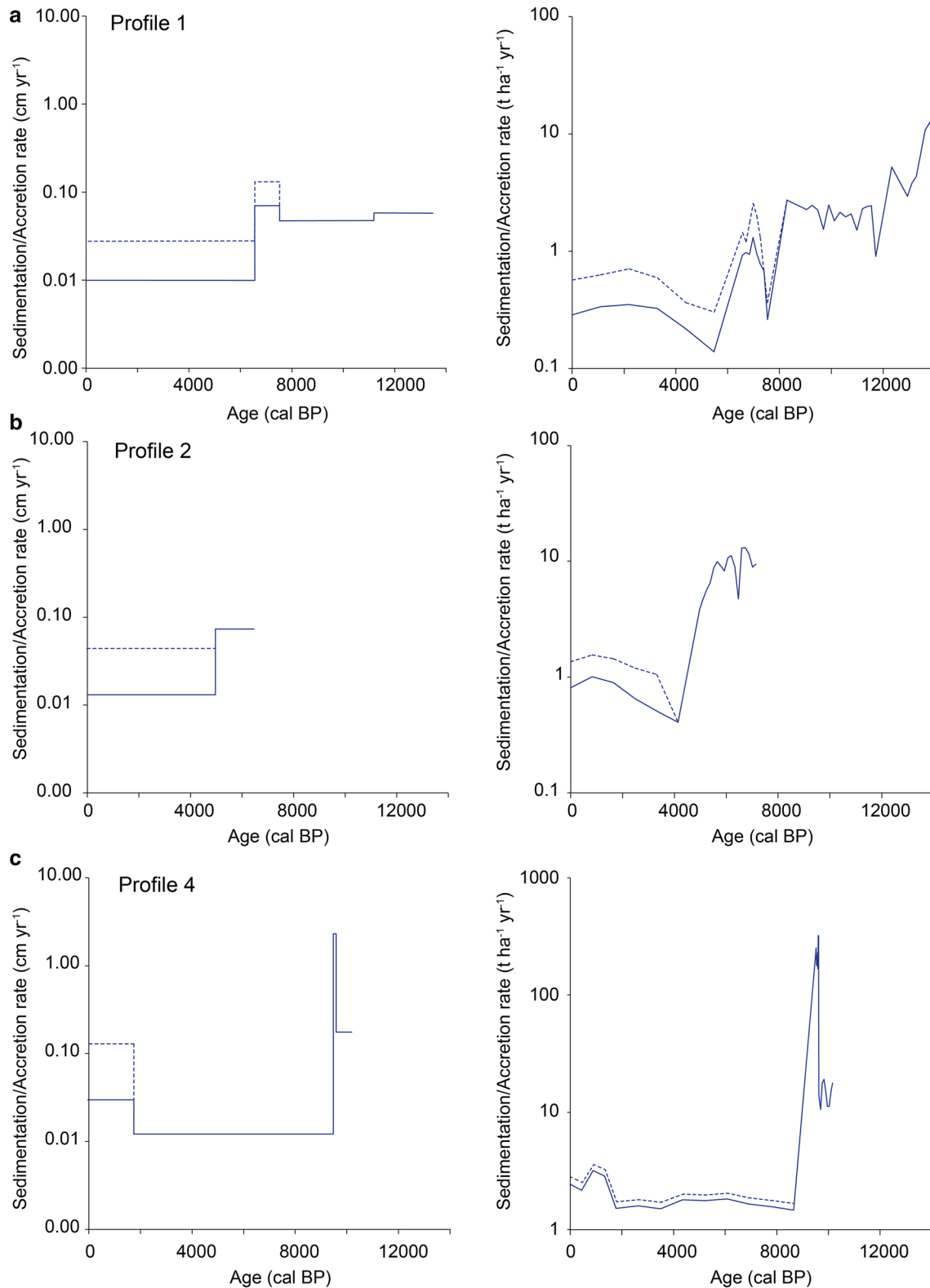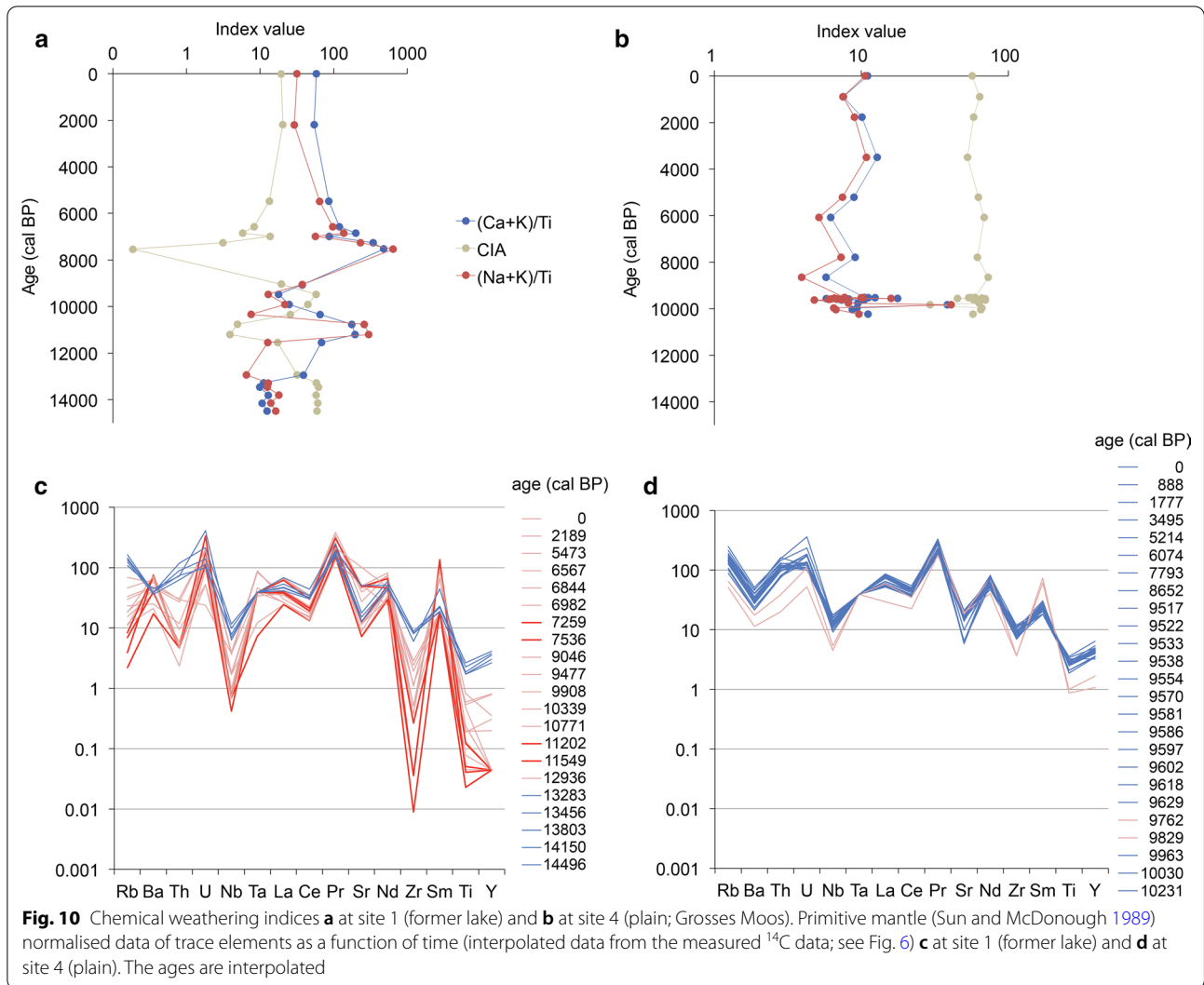
Fig. 9 Sedimentation or accretion rates as a function of time at the sites **a** 1, **b** 2 and **c** 4. The rates are plotted as cm year^{-1} (including, thus, a length unit) and as t ha^{-1} year^{-1} (including a weight unit; the depth- and thus time-dependent bulk density of the deposited/accreted material was taken into account). The dotted lines indicate the sedimentation or accretion rates if no degradation of mires had taken place

Fig. 10 Chemical weathering indices **a** at site 1 (former lake) and **b** at site 4 (plain; Grosses Moos). Primitive mantle (Sun and McDonough 1989) normalised data of trace elements as a function of time (interpolated data from the measured ^{14}C data; see Fig. 6) **c** at site 1 (former lake) and **d** at site 4 (plain). The ages are interpolated

Aare river was the main source of material supply. With respect to the trace elements, the variability of the deposited material at profile 1 seems relatively large. Several phases having a moderately comparable composition can be distinguished: 13–11 ka BP, 11–9 ka BP, 9–7 ka PB and 7 ka BP to today.

5 Discussion

5.1 Mire development, geomorphic activity and landscape evolution

The investigated sites exhibit a distinct variability in terms of profile composition and ages. Profile 1 can be ascribed to a former lake that started to increasingly silt around 13.5 ka BP. With increasing sedimentation of this former lake, a bog started to form around 10 ka BP. The sites 2–4 are all near the former stream courses of the Aare river. As a consequence, the profile compositions

reflect the meandering behaviour and the sediment loads of the former Aare river (Wohlfarth-Meyer 1987). The formation of some rather shallow mires started in the period from 10 to 3 ka BP. Due to the meandering of the Aare river, the formation of mires was spatio-temporally patchy (Fig. 6). The sites S, P33, S1 and S2 are closer to the lake of Neuchâtel and represent the formation of peat close to a lake that over time lost part of its volume.

Based on the age-depth trends, sedimentation/accretion rates could be calculated for some of the sites. Similar to other investigations (Raab et al. 2019), the transition from Late Pleistocene environmental conditions to those of the Holocene was characterised by distinct phases of both erosion and sedimentation. A moderately similar situation seems to have occurred also in the Swiss Plateau (Swiss canton of Berne), where sedimentation rates were distinctly increased during the Late Pleistocene and

Early Holocene compared to the Middle or Late Holocene (Fig. 9). The transition from the Pleistocene to the Holocene was characterised by abrupt climate changes, increased precipitation and partially still-scarce vegetation causing increased erosion and sedimentation. At the end of the Pleistocene, probably during the Younger Dryas period, periglacial processes, solifluction and mixing with loess loam prevailed on slopes (Mailänder and Veit 2001). The results of Veit et al. (2017) indicate strong morphodynamic activities during the early Holocene up to c. 7.5 ka BP, suggesting an open landscape in the investigation area. During the Early Holocene, prior to 7.5 ka, slope wash with linear erosion occurred. Later, the erosion rills were filled up with the removed Pleistocene loess loam available on the slopes (Veit et al. 2017).

In addition, in the early Holocene, several rapid climatic changes were reported around 11.1, 10.3 and 9.4 ka BP (Florescu et al. 2019) contributing to high sediment loads of rivers. This also agrees with the findings of Wohlfarth and Schneider (1991). During the Allerød, Younger Dryas and beginning of the Preboreal, relatively-quiet hydrodynamic conditions seemed to prevail in the lake of Biel. Between the Preboreal and Atlantic, a higher fluctuation of the lake level and, thus, a higher hydrodynamic environment is reported (Wohlfarth and Schneider 1991). From the Younger Atlantic to the Subboreal, again relatively-quiet hydrodynamic conditions were measured in the lake of Biel. According to Veit et al. (2017), the landscape stabilised and soils developed after 7.5 ka together with the spread of woodland and reduced seasonal contrasts. This corresponds with the lower sedimentation rates found at c. 5 to 2 ka BP (profile 2) and c. 8 to 2 ka BP (profile 4) (Fig. 9).

The geoforensic approach indicates that major disturbances occurred from 12 to c. 7 ka BP. It also suggests that larger regions than today were hydrologically connected until c. 13 ka BP. The hydrological connection between profile 1 and 3 must have been interrupted c. 13 ka BP. Since then, the pattern of profile 1 seems to reflect predominantly local characteristics; i.e. material that was deposited in the lake such as lake marl or lake clays. Part of this material derives from erosion of the local soils and sediments. Additional small and/or larger lakes existed in Three Lakes Region at that time (Wohlfarth-Meyer 1990; Ledermann 1991).

Archaeologically, the Neolithic period in Switzerland is dominated by lakeshore and bog settlement sites having organic preservation, the occupation of inner Alpine sites of the Rhône valley and high mountain pass sites (Siebke et al. 2019). Archaeological finds are particularly numerous in the region of Lake Zurich in Eastern Switzerland and the Three Lakes Region in Western Switzerland (Furtwängler et al. 2020). During the Early Bronze Age,

the landscape was more and more influenced by human impact due to clearing of forests and increasing use of agricultural land. Until the Roman period, fewer inundations occurred in the region of interest. This was also due to a change of the stream course of the Aare river (for the last 3–5 kyr the draining has occurred mostly in northern direction; Fig. 11). In part, a productive agriculture was possible during this period (Haas et al. 2019).

During the last 2000 years however, higher sedimentation rates—caused again by an increasing number of inundations—were recorded. The climatic conditions became harsher, particularly during the Little Ice Age (LIA). Moreover, the pre-existence of forest clearing contributed to the again increased erosion and sedimentation dynamics (Makri et al. 2020).

5.2 Carbon losses since the first Jura Swiss water-level optimisations

Owing to the water-level optimisations carried out in the nineteenth and twentieth centuries, intense draining and land use, surface lowering of the former mires was distinct with the result that larger areas today have only a thin organic soil layer (degraded peat). For the period of approximately the last 150 years, we were able to conclude there was an annual C loss in agricultural land in the range of c. 5 t ha^{-1} and about half of that occurring in forested areas. These values match well with reported C losses in agricultural land where maximum rates were even up to 11.2 t ha^{-1} year^{-1} (Byrne et al. 2004; Höper 2007; Grønlund et al. 2008; Kirk et al. 2015). In the literature, there seems to be a disagreement about the effects of a change of mires into forests. Some investigations show that additional organic matter (e.g. Hargreaves et al. 2003) is sequestered while others demonstrate that C-losses may occur (Byrne et al. 2004; Byrne und Farrell 2005; Höper 2007). Depending on the climate (particularly tropical regions) and environmental conditions, particularly drainage depth, very high C-losses were reported (Vaidyanathan 2011; Matysek et al. 2018). Due to the cool climate and a shallow drainage system that is often only 20–30 cm deep, some boreal forest peatlands may gain C after drainage—the improved plant growth and hence higher net primary production outweighs the C loss from peat oxidation (Hargreaves et al. 2003). Afforested peatlands in Scotland accumulated more carbon in trees, litter and soil than was lost from the peat.

In temperate to boreal climate zones, C-losses seem in general lower when mires are transformed into a forest instead of agricultural land. For example, Minkkinen et al. (2008) measured a lower subsidence rate under forest than in agricultural land. However, it cannot be denied that even with forestry, mire will degrade in the mid-term (cf. Ojanen et al. 2013), though the rate of
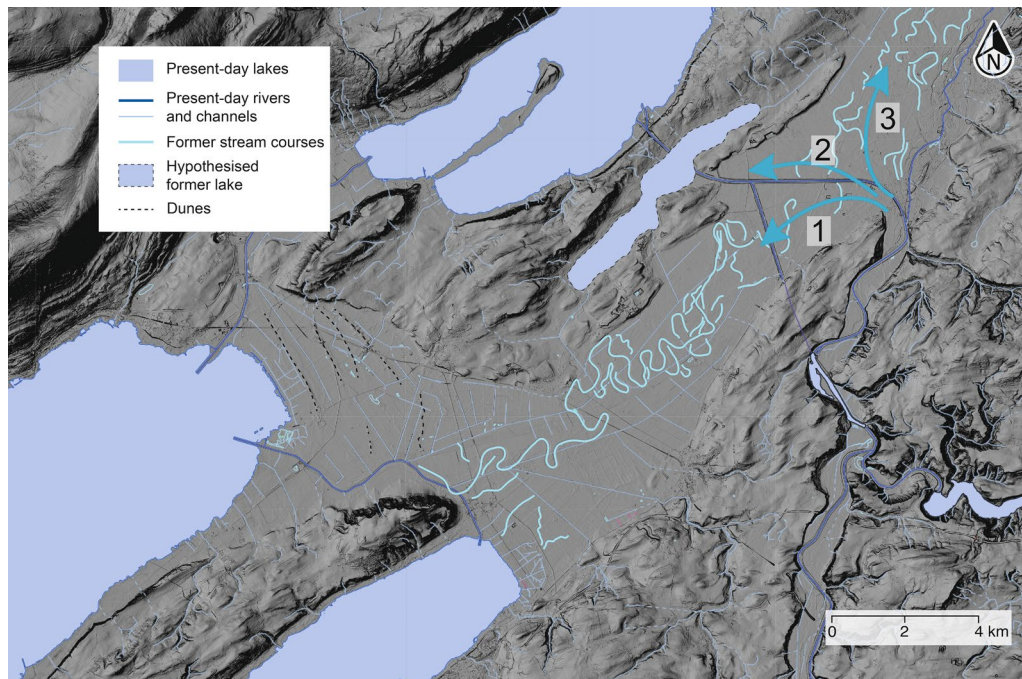
Fig. 11 Former stream courses of the Aare river in direction to the lake of Neuchâtel (1) until about 5 ka BP (Wohlfarth-Meyer 1987), (2) hydrological connection of the Aare river with the former lake in western part of the main plain (Grosses Moos) until about 13 ka BP and (3) main drain of the Aare river for about the last 3–5 kyr. Note also the former extension of the lake of Neuchâtel (dunes) (Source: SwissALTI3D swisstopo)

degradation is slower. Our results on C-losses from the Three Lakes Region concur with estimates on losses from forests on drained bogs in the pre-Alps of Switzerland (Wüst-Galley et al. 2016).

To reduce the ongoing peat degradation process, related CO_2 emissions and surface subsidence, new land use strategies are currently discussed or were suggested. Among them are the cultivation of rice (paludiculture; Gramlich et al. 2020) or agroforestry. Paludiculture should reduce peat decomposition or may even contribute to its formation (Wichtmann et al. 2010). Agroforestry would not completely stop peat decay but may contribute to a much slower degradation and contribute to humus stabilisation (Wiesmeier et al. 2017).

6 Conclusions

The mires of the Three Lakes Region (Swiss canton of Berne) started to form earliest c. 10 ka BP. In the valley floor of the 'Grosses Moos', the meandering Aare river gave rise to a spatio-temporally patchy formation of mires. Some of these mires developed after the silting up of lakes, or in vicinity to lakes that flooded from time to time. Consequently, the thickness of the mire and organic matter content varies as a function of the environmental settings. Until c. 13 ka BP larger regions were hydrologically connected to each other. An additional lake must have existed to the western end of the plain which most likely also received sediments from the Aare river. At c. 13 ka BP, this lake was cut off from a hydrological connection to the Aare river. The lake was finally silted up at c. 10 ka BP.

The transition period from the Pleistocene to the Holocene is characterised by high sedimentation rates in the plain. Due to strong morphodynamic activities during the Late Pleistocene/Early Holocene, high erosion and sedimentation rates and a high variability in the chemical composition of the material were recorded until up to c. 7.5 ka BP. The situation remained in part quiet between c. 5 and 2 ka BP (also due to a change of the drain of the Aare river). During the last about 2 kyr, the hydrodynamic and geomorphic activities were increased again.

With the optimisation of the water-levels of the Three Lakes Region (Swiss Jura water-level optimisation), peat bogs and swamps were transformed into arable land during the nineteenth and twentieth century. Since then, the mires have been degraded strongly. Average annual C-losses in agricultural land are c. 4.9 t ha^{-1} and in forests c. 2.4 t ha^{-1}. Surface lowering at the sites where C-budget calculations were possible lie in the range of 76 to 249 cm within about 150 years.

The aggradation of the mires and bogs was a process occurring over several millennia—their partially complete degradation has now occurred during the last 150 years. Although the interventions to regulate the water-levels undoubtedly brought an improvement of the livelihood of the local population and extirpated malaria, new land use concepts are needed to prevent landscape and soil destruction and to reduce unwanted CO_2 emissions caused by the mineralisation of soil organic matter. In addition to ongoing experiments with rice cultivation (paludiculture), different types of agroforestry might be tested as alternative land use systems, although forests only limit, but do not stop the degradation of mires.

Supplementary information

Supplementary information accompanies this paper at https://doi.org/10.1186/s00015-020-00376-0.

Additional file 1: Table S1. Physical characteristics, LOI (loss on ignition) and organic C of the investigated samples.

Additional file 2: Table S2. Total chemical composition of the investigated samples.

Author details
[1] Department of Geography, University of Zürich, 8057 Zurich, Switzerland. [2] Agroscope, Reckenholzstrasse 191, 8046 Zurich, Switzerland. [3] Swiss Federal Research Institute WSL, Zürcherstrasse 111, 8903 Birmensdorf, Switzerland.

References
Bajard, M., Poulenard, J., Sabatier, P., Develle, A. L., Giguet-Covex, C., Jacob, J., et al. (2017). Progressive and regressive soil evolution phases in the Anthropocene. *CATENA, 150,* 39–52.

Birks, H. H., & Birks, H. J. B. (2001). Future uses of pollen analysis must include plant macrofossils. *Journal of Biogeography, 27,* 31–35.

Blaauw, M. (2010). Methods and code for "classical" age-modelling of radiocarbon sequences. *Quaternary Geochronology, 5,* 512–518.

Brisset, E., Miramont, C., Guiter, F., Anthony, E., Tachikawa, K., Poulenard, J., et al. (2013). Non-reversible geosystem destabilisation at 4200 cal. BP: Sedimentological, geochemical and botanical markers of soil erosion recorded in a Mediterranean alpine lake. *The Holocene, 23,* 1863–1874.

Burga, C. A., & Perret, R. (1998). *Vegetation und Klima der Schweiz seit dem jüngeren Eiszeitalter.* Thun: Ott Verlag.

Byrne, K. A., Chojnicki, B., Christensen, T. R., Drösler, M., Freibauer, A., Frolking, S., et al. (2004). *EU Peatlands: Current carbon stocks and trace gas fluxes* (pp. 1–58). Viterbo: Department of Forest Science and Environment.

Byrne, K. A., & Farrell, E. (2005). The effect of afforestation on soil carbon dioxide emissions in blanket peatland in Ireland. *Forestry, 3,* 217–227.

Derakhshan-Babaei, F., Nosrati, K., Tikhomirov, D., Christl, M., Sadough, H., & Egli, M. (2020). Relating the spatial variability of chemical weathering and erosion to geological and topographical zones. *Geomorphology, 363,* 107235.

Florescu, G., Brown, K. J., Carter, V. A., Kuneš, P., Veski, S., & Feurdean, A. (2019). Holocene rapid climate changes and ice-rafting debris events reflected in high-resolution European charcoal records. *Quaternary Science Reviews, 222,* 105877.

Furtwängler, A., Rohrlach, A. B., Lamnidis, T. C., Papac, L., Neumann, G. U., Siebke, I., et al. (2020). Ancient genomes reveal social and genetic structure of Late Neolithic Switzerland. *Nature Communications, 11,* 1915.

Gramlich, A., Churko, G., Jacot, K., & Walter, T. (2020). Biodiversität auf Nassreisfeldern im Schweizerischen Mittelland: Gefährdete Arten finden neuen Lebensraum. Resultate der Pilotphase 2019. *Agroscope Transfer, 332,* Retrieved from https://ira.agroscope.ch/de-CH/publication/44139.

Grønlund, A., Hauge, A., Hovde, A., & Rasse, D. P. (2008). Carbon loss estimates from cultivated peat soils in Norway: A comparision of three methods. *Nutrient Cycling in Agroecosystems, 81,* 157–167.

Grünig, A. (2007). Moore und Sümpfe im Wandel der Zeit. *Hotspot, 15,* 4–5.

Haas, M., Baumann, F., Castella, C., Haghipour, N., Reusch, A., Strasser, M., et al. (2019). Roman-driven cultural eutrophication of Lake Murten, Switzerland. *Earth and Planetary Science Letters, 505,* 110–117.

Hargreaves, K. J., Milne, R., & Cannell, M. G. R. (2003). Carbon balance of afforested peatland in Scotland. *Forestry, 76,* 299–317.

Höper, H. (2007). Freisetzung von Treibhausgasen aus deutschen Mooren. *Telma, 37,* 85–116.

Ivy-Ochs, S., Kerschner, H., Reuther, A., Maisch, M., Sailer, R., Schaefer, J., et al. (2006). The timing of glacier advances in the northern European Alps based on surface exposure dating with cosmogenic 10Be, 26Al, 36Cl, and 21Ne. *Special Paper of the Geological Society of America, 415,* 43–60.

Ivy-Ochs, S., Kerschner, H., Reuther, A., Preusser, F., Heine, K., Maisch, M., et al. (2008). Chronology of the last glacial cycle in the European Alps. *Journal of Quaternary Science, 23,* 559–573.

Jäger, H., Achermann, M., Waroszewski, J., Kabala, C., Malgorzata, M., Gärtner, H., et al. (2015). Mire sediments as a mirror of erosion and soil formation. *CATENA, 128,* 63–79.

Kirk, E. R., van Kessel, C., Horwath, W. R., & Linquist, B. A. (2015). Estimating annual soil carbon loss in agricultural peatland soils using a nitrogen budget approach. *PLoS ONE, 10,* e0121432.

Klaus, G. (2007). *Zustand und Entwicklung der Moore in der Schweiz. Ergebnisse der Erfolgskontrolle Moorschutz.* Umwelt-Zustand Nr. 0730. Bundesamt für Umwelt, Bern.

Ledermann, H. (1991). Über den «Solothurnersee». *Mitteilungen der Naturforschenden Gesellschaft Solothurn, 35,* 213–231.

Leifeld, J., Gubler, L., & Grünig, A. (2011). Organic matter losses from temperate ombrotrophic peatlands: An evaluation of the ash residue method. *Plant and Soil, 341,* 349–361.

Leifeld, J., Klein, K., & Wüst-Galley, C. (2020). Soil organic matter stoichiometry as indicator for peatland degradation. *Scientific Reports, 10,* 7634.

Lienert, B. (2013). *Einfluss von Aufforstungen auf Kohlenstoffverluste aus organischen Böden (Halbmooren) im Staatswald bei Witzwil (BE).* MSc thesis, University of Zurich, Zurich.

Limpens, J., Berendse, F., Blodau, C., Canadell, J. G., Freeman, C., Holden, J., et al. (2008). Peatlands and the carbon cycle: From local processes to global implications—A synthesis. *Biogeosciences, 5,* 1475–1491.

Mailänder, R., & Veit, H. (2001). Periglacial cover-beds on the Swiss Plateau: Indicators of soil, climate and landscape evolution during the Late Quaternary. *CATENA, 45,* 251–272.

Makri, S., Rey, F., Gobet, E., Gilli, A., Tinner, W., & Grosjean, M. (2020). Early human impact in a 15.000-year high-resolution record of paleoproduction and anoxia from a varved lake in Switzerland. *Quaternary Science Reviews, 239,* 106335. https://doi.org/10.1016/j.quascirev.2020.106335.

Malmer, N., & Holm, E. (1984). Variation in the C/N quotient of peat in relation to decomposition rate and age determination with PB-210. *Oikos, 43,* 171–182.

Matysek, M., Evers, S., Samuel, M. K., & Sjogersten, S. (2018). High heterotrophic CO_2 emissions from a Malaysian oil palm plantations during dry-season. *Wetlands Ecology and Management, 26,* 415–424.

Minkkinen, K., Byrne, K. E., & Trettin, C. (2008). Chapter 4, Climate impacts of peatland forestry. In M. Strack (Ed.), *Peatlands and climate change* (pp. 98–122). Jyväskylä: International Peat Society.

Moser, W. (1991). Die erste und die zweite Juragewässerkorrektion 1868–1891;1962–1973. *Jahrbuch für solothurnische Geschichte, 64,* 225–294.

Mourier, B., Poulenard, J., Carcaillet, C., & Williamson, D. (2010). Soil evolution and subalpine ecosystem changes in the French Alps inferred from geochemical analysis of lacustrine sediments. *Journal of Paleolimnology, 44,* 571–587.

Nast, M. (2006). *Überflutet – überlebt – überlistet Die Geschichte der Juragewässerkorrektionen.* Nidau: Verein Schlossmuseum Nidau.

Nesbitt, H. W., & Young, G. M. (1982). Early Proterozoic climates and plate motions inferred from major element chemistry of lutites. *Nature, 299,* 715.

Ojanen, P., Minkkinen, K., & Penttil, T. (2013). The current greenhouse gas impact of forestry drained boreal peatlands. *Forest Ecology and Management, 289,* 201–208.

Pitkänen, A., Simola, H., & Turunen, J. (2012). Dynamics of organic matter accumulation and decomposition in the surface soil of forestry-drained peatland sites in Finland. *For Ecol Manag, 284,* 100–106.

Preusser, F. (2004). Towards a chronology of the Late Pleistocene in the northern Alpine Foreland. *Boreas, 33,* 195–210.

Preusser, F., Blei, A., Graf, H. R., & Schlüchter, C. (2007). Luminescence dating of Würmian (Weichselian) proglacial sediments from Switzerland: Methodological aspects and stratigraphical conclusions. *Boreas, 36,* 130–142.

Raab, G., Egli, M., Norton, K., Dahms, D., Brandová, D., Christl, M., et al. (2019). Climate and relief-induced controls on the temporal variability of denudation rates in a granitic upland. *Earth Surface Processes and Landforms, 44,* 2570–2586.

Raab, G., Halpern, D., Scardiglia, F., Raimondi, S., Norton, K., Pettke, T., et al. (2017). Linking tephrochronology and soil characteristics in the Sila and Nebrodi Mountains, Italy. *CATENA, 158,* 266–285.

Reimer, P. J., Bard, E., Bayliss, A., Beck, J. W., Blackwell, P. G., Bronk Ramsey, C., et al. (2013). IntCal13 and Marine13 radiocarbon age calibration curves 0–50,000 years cal BP. *Radiocarbon, 55,* 1869–1887.

Schlüchter, C. (2004). The Swiss glacial record—A schematic summary. In J. Ehlers & P. L. Gibbard (Eds.), *Quaternary glaciations—Extent and chronology* (pp. 413–418). Amsterdam: Elsevier.

Siebke, I., Steuri, N., Furtwängler, A., Ramstein, M., Arenz, G., Hafner, A., et al. (2019). Who lived on the Swiss Plateau around 3300 BCE? Analyses of commingled human skeletal remains from the dolmen of Oberbipp. *International Journal of Osteoarchaeology, 29,* 786–896.

Stiles, C. A., Mora, C. I., & Driese, S. G. (2003). Pedogenetic processes and domain boundaries in a vertisol climosequence: Evidence from titanium and zirconium distribution and morphology. *Geoderma, 116,* 279–299.

Sun, S. S., & McDonough, W. F. (1989). Chemical and isotopic systematics of oceanic basalts implications for mantle composition and processes. Geological Society Special Publication 42. In A. Saunders & M. J. Norry (Eds.), *Magmatism in the ocean basins* (pp. 313–345). Oxford: Blackwell Scientific.

Tinner, W., & Theurillat, J.-P. (2003). Uppermost limit, extent, and fluctuations of the timberline and treeline ecocline in the swiss central Alps during the past 11,500 years. *Arctic Antarctic and Alpine Research, 35,* 158–169.

Vaidyanathan, G. (2011). Counting the carbon cost of peatland conversion. *Nature.* https://doi.org/10.1038/news.2011.139.

Veit, H., Trauerstein, M., Preusser, F., Messmer, T., Gnägi, C., Zech, R., et al. (2017). Late Glacial/Early Holocene slope deposits on the Swiss Plateau: Genesis and palaeo-environment. *CATENA, 158,* 102–112.

Vischer, D., & Feldmann, H.-U. (2005). Die erste Juragewässerkorrektion, 1868–1891. *Cartographica Helvetica, 32,* 17–32.

Wang, M., Moore, T. R., Talbot, J., & Riley, J. L. (2015). The stoichiometry of carbon and nutrients in peat formation. *Global Biogeochemical Cycles, 29,* 113–121.

Wichtmann, W., Tanneberger, F., Wichmann, S., & Joosten, H. (2010). Paludiculture is paludifuture: Climate, biodiversity and economic benefits from agriculture and forestry on re-wetted peatland. *Peatlands International, 1,* 48–51.

Wiesmeier, M., Burmeister, J., Treisch, M., & Brandhuber, R. (2017). Klimaschutz durch Humusaufbau—Umsetzungsmöglichkeiten der 4 Promille-Initiative in Bayern. In: *Bayerische Landesanstalt für Landwirtschaft (LfL), Landwirtschaft im Klimawandel Lösungen, die Geld sparen,* pp. 21–30.

Wohlfarth, B., & Schneider, A. M. (1991). Late Glacial and Holocene lake level fluctuations in Lake Biel, Western Switzerland. *Journal of Quaternary Science, 6,* 293–302.

Wohlfarth-Meyer, B. (1987). Lithostratigraphische, sedimentologische und chronologische Untersuchungen im Quartär des Schweizer Seelandes (Kantone Bern und Fribourg). *Eclogae Geologicae Helvetiae, 80,* 207–222.

Wohlfarth-Meyer, B. (1990). Der Solothurnersee: ein geologischer Mythos? In J. Schibler, J. Sedlmeier, & H. Spycher (Eds.), *Festschrift für Hans R* (pp. 319–325). Basel: Stampfli. Helbling & Lichtenhahn.

Wüst-Galley, C., Grünig, A., & Leifeld, J. (2020). Land use-driven historical soil carbon losses in Swiss peat-lands. *Landscape Ecology, 35,* 173–187.

Wüst-Galley, C., Mössinger, E., & Leifeld, J. (2016). Loss of the soil carbon function of drained forested peatlands. *Mires and Peat, 18,* 1–22.

Wüthrich, L., Morabito, E. G., Zech, J., Trauerstein, M., Veit, H., Gnägi, C., et al. (2018). [10]Be surface exposure dating of the last deglaciation in the Aare Valley, Switzerland. *Swiss Journal of Geosciences, 111,* 295–303.

Zanon, M., Davis, A. S., Marquer, L., Brewer, S., & Kaplan, J. O. (2018). European forest cover during the past 12,000 years: A palynological reconstruction based on modern analogs and remote sensing. *Frontiers in Plant Science.* https://doi.org/10.3389/fpls.2018.00253.

Zihlmann, U., Weisskopf, P., Müller, M., Freund, M., Hirschi, M., Chervet, A., et al. (2019). Entwässerte, landwirtschaftlich genutzte Torfböden beurteilen und nach Bedarf aufwerten. In S. Spielvogel & C. Ahl (Eds.), *Exkursionsführer Bern, DBG Band 119* (pp. 163–178). Bern: S. Spielvogel.

Publisher's Note